Available online at www.sciencedirect.com

ScienceDirect

Journal of Taibah University for Science 11 (2017) 548–565

Journal of Taibah University for Science

www.elsevier.com/locate/jtusci

Reynold's model viscosity on radiative MHD flow in a porous medium between two vertical wavy walls

A.B. Disu [a,*], M.S. Dada [b]

[a] *School of Science and Technology, National Open University of Nigeria, Victoria Island, Lagos, Nigeria*
[b] *Department of Mathematics, University of Ilorin, Ilorin, Nigeria*

Received 26 May 2015; received in revised form 16 July 2015; accepted 5 December 2015
Available online 21 December 2015

Abstract

The two dimensional heat transfer of a free convective–radiative MHD (magnetohydrodynamics) flows with variable viscosity and heat source of a viscous incompressible fluid in a porous medium between two vertical wavy walls was investigated. The fluid viscosity is assumed to vary as an exponential function of temperature. The flow is assumed to consist of a mean part and a perturbed part. The perturbed quantities were expressed in terms of complex exponential series of plane wave equation. The resultant differential equations governing the flow were non-dimensionalised and solved using Differential Transform Method (DTM). The numerical computations were presented in tabular and graphical forms for various fluid parameters. It shows that an increase in radiation, variable viscosity and permeability parameters cause a rise in velocity profile. Nusselt number increases with increase in heat source and decreases with increase in radiation parameter at both walls.

MSC: 76S05; 76W99

Keywords: Wavy walls; Porous medium; Reynold's model viscosity; Two-dimensional radiation; Differential Transform Method

1. Introduction

The study of viscous fluid flow over wavy wall(s) has received considerable attention of researchers due to its applications in nature and engineering such as in designing ventilated heating building, electronic components cooling and as well as in designing blood oxygenator and drying of several types of agricultural products (grain and food). In recent years, the interest of some researchers has been drawn to the study of fluid flow in the area of physiological processes through wavy channels. In particular, the peristaltic flow in the vasomotion of small blood vessels such as

* Corresponding author. Tel.: +234 8077138381.
E-mail addresses: adisu@noun.edu.ng (A.B. Disu), msadada@unilorin.edu.ngg (M.S. Dada).
Peer review under responsibility of Taibah University.

Production and hosting by Elsevier

http://dx.doi.org/10.1016/j.jtusci.2015.12.001

arterioles, venules, and capillaries, urine transport from kidney to bladder, spermatozoa transport in the ducts efferent of the male reproductive tract and in the cervical canal, transport of lymph in the lymphatic vessels, movement of ovum in the female fallopian tube and swallowing food through the oesophagus [1–7].

The theoretical and practical significance of the viscous fluid over wavy wall(s) were discussed by Lekoudis et al. [8], Shankar and Sinha [9], Lessen and Gangwani [10], Vajravelu and Sastri [11] and Das and Ahmed [12]. In the studies, the authors had given special attention to the wavines on the fluid flow and heat transfer characteristics.

The fluid flow through wavy channel is often used in certain engineering processes like glass manufacturing, crude oil refinement, paper production and in some geophysical studies under the influence of magnetic field [6,7]. The influence of magnetic field on corrugated channel was presented by Fasogbon [13] and it was reported that the magnetic field intensity slowed down the fluid motion. Tak and Kumar [14] investigated the heat transfer with radiation in the MHD free convection between a vertical wavy wall and a parallel flat wall. The authors presented that the thermal radiation speed up the velocity of the fluid. Fasogbon [15] considered the effects of mass transfer in irregular the channel and concluded that different chemical species enhance the velocity of the fluid. In the same vein, Abubakar [16] investigated natural convective flow and heat transfer in a viscous incompressible fluid with slip effect confined within spirally-enhanced channel and reported that the slip had a linear effect on the fluid motion. All these studies were narrowed down to one vertical wavy wall with a parallel flat wall.

The study of MHD free convection flow between two vertical wavy walls was studied by Tak and Kumar [17] and Kumar [18]. The authors noticed for non porous medium that viscous dissipation and thermal radiation had a linear accelerating effect on the fluid flow while the magnetic field intensity and heat source had a retarding effect on the fluid motion.

The study of fluid flow in a porous medium is significant because of its applications in soil mechanics, water purification, underground water hydrology, chemical engineering, petroleum engineering, ceramic engineering, metallurgical engineering, agricultural engineering and water irrigation process. Hence, Adesanya and Makinde [19], Makanda et al. [20] and Das et al. [21] had studied the fluid flow in a porous medium between two parallel flat walls.

However, the study of the fluid flow in a porous between two wavy walls has received relatively less attention. Among the studies, Teneja and Jain [22] investigated the MHD free convection flow in the presence of a temperature dependent heat source in a viscous incompressible fluid confined between a long vertical wavy wall and a parallel flat wall in slip flow regime with constant heat flux at the flat wall through a porous medium between vertical wavy walls. Dada and Disu [23] studied the heat transfer with radiation and temperature dependent heat source in a porous medium between two vertical wavy walls. It was reported that the velocity of the fluid increases with the increase in the permeability of the porous medium.

In all the above-mentioned studies, viscosity of the fluid was assumed to be constant. However, It is a known fact that viscosity property varies significantly with temperature [24]. For lubricating fluids, heat generated by the internal friction and the corresponding rise in temperature affects the viscosity of the fluid. Hence, assuming a uniform viscosity throughout the fluid flow regime may not represent the physical reality of the flow.

As a result, the present study investigates the Reynold's model (temperature dependent) viscosity on a radiative MHD free convection flow in a porous medium between two vertical wavy walls. To achieve the aim of this study, perturbation technique coupled with Differential Transform Method was used to obtain the set of solutions of non-linear differential equations.

2. Formulation of the problem

Consider a steady laminar natural convective hydromagnetic flow in a porous medium between a long vertical wavy channel. The X-axis is vertically upwards while Y-axis is perpendicular to it. The wavy walls are represented by $Y=\varepsilon^*\cos(\Lambda X)$ and $Y=a+\varepsilon^*\cos(\Lambda X)$ respectively, where $\varepsilon^* \ll 1$, and Λ is the amplitude of the wavy walls. The equations governing the steady flow and heat transfer with temperature dependent heat source are as follows:

$$\rho\left(U\frac{\partial U}{\partial X}+V\frac{\partial U}{\partial Y}\right)=-\frac{\partial P}{\partial X}+\frac{\partial}{\partial X}\left(\mu(T)\frac{\partial U}{\partial X}\right)+\frac{\partial}{\partial Y}\left(\mu(T)\frac{\partial U}{\partial Y}\right)+g\beta(T-T_c)-H_0^2U-\frac{\mu(T)}{K^*}U, \tag{1}$$

$$\rho\left(U\frac{\partial V}{\partial X}+V\frac{\partial V}{\partial Y}\right)=-\frac{\partial P}{\partial Y}+\frac{\partial}{\partial X}\left(\mu(T)\frac{\partial V}{\partial X}\right)+\frac{\partial}{\partial Y}\left(\mu(T)\frac{\partial V}{\partial Y}\right)-\frac{\mu(T)}{K^*}V, \tag{2}$$

$$\frac{\partial U}{\partial X}+\frac{\partial V}{\partial Y}=0, \tag{3}$$

$$\rho C_p\left(U\frac{\partial T}{\partial X}+V\frac{\partial T}{\partial Y}\right)=k\left(\frac{\partial^2 T}{\partial X^2}+\frac{\partial^2 T}{\partial Y^2}\right)-\frac{\partial q_x}{\partial X}-\frac{\partial q_y}{\partial Y}+Q(T_c-T), \tag{4}$$

with the following boundary conditions:

$$\left.\begin{aligned} &U=0,\quad V=0,\quad T=T_c,\quad \text{at}\quad Y=\varepsilon^*\cos(\Lambda X),\\ &U=0,\quad V=0,\quad \frac{\partial T}{\partial Y}=0,\quad \text{at}\quad Y=a+\varepsilon^*\cos(\Lambda X),\end{aligned}\right\} \tag{5}$$

where U, V are the velocity components, P is the pressure, μ is the dynamic viscosity, β is the coefficient of volume expansion, H_0^2 is the uniform magnetic field, K^* is the porosity parameter, k is the thermal conductivity, ρ is the density of the fluid, c_p is the specific heat at constant pressure, Q is the temperature dependent heat source and T_c is the equilibrium temperature. Also, q_x is radiative heat flux in the X-direction and q_y is radiative heat flux in the Y-direction (Ozisik [25]).

Following Rosseland approximation (Brewster [26]) the radiative heat flux in the X- and Y-directions respectively can be expressed

$$q_x=-\frac{4\sigma\partial T^4}{3R\partial X},\quad q_y=-\frac{4\sigma\partial T^4}{3R\partial Y}, \tag{6}$$

where σ is the Stefan–Boltzmann constant and a_R is the mean absorption coefficient. If the temperature differences within the flow are small such that T^4 can be expressed as a series of its temperature, then the Taylor series T^4 about T_c, neglecting higher order terms, is

$$T^4=4T_c^3T-3T_c^4. \tag{7}$$

The fluid viscosity in Eqs. (1) and (2) is assumed to vary exponentially as function of temperature (Reynold's model viscosity). The form of the viscosity can be expressed as

$$\mu(T)=\mu e^{-B(T-T_c)}, \tag{8}$$

where μ is the fluid viscosity at reference temperature T_c and B is the strength of dependency between $\mu(T)$ and T. The Reynold's viscosity decreases or increases with an increase in temperature for liquid or gas.

The following dimensionless parameters are used for Eqs. (1)–(8)

$$\left.\begin{aligned} &(x,y)=\frac{1}{a}(X,Y),\quad (u,v)=\frac{a}{\nu}(U,V),\quad p=\frac{Pa^2}{\rho\nu^2},\quad \theta=\frac{T-T_c}{T_c-T_s},\quad Pr=\frac{\mu c_p}{k},\\ &\gamma=B(T_c-T_s),\quad G=\frac{g\rho\beta a^4}{k\nu^2},\quad R=\frac{ka_R}{4\sigma T_c^3},\quad \alpha=\frac{Qa^2}{k},\quad M=\frac{H_0a^2}{\rho\nu},\quad K=\frac{K^*}{\nu a^2},\quad \lambda=\Lambda a,\quad \varepsilon=\frac{\varepsilon^*}{a},\end{aligned}\right\} \tag{9}$$

where γ is the variable viscosity parameter, G is the Grashof number, Pr is the Prandtl, α is the heat source parameter, M is the magnetic parameter, R is radiation parameter, K is the porosity parameter, λ is the dimensionless frequency and ε is the dimensionless amplitude ratio.

Eqs. (1)–(5) in dimensionless form reduce to

$$u\frac{\partial u}{\partial x}+v\frac{\partial u}{\partial y}=-\frac{\partial p}{\partial x}+\frac{\partial}{\partial x}\left(e^{-\gamma\theta}\frac{\partial u}{\partial x}\right)+\frac{\partial}{\partial y}\left(e^{-\gamma\theta}\frac{\partial u}{\partial y}\right)+G\theta-Mu-\frac{e^{-\gamma\theta}}{K}u, \tag{10}$$

$$u\frac{\partial v}{\partial x}+v\frac{\partial v}{\partial y}=-\frac{\partial p}{\partial y}+\frac{\partial}{\partial x}\left(e^{-\gamma\theta}\frac{\partial v}{\partial x}\right)+\frac{\partial}{\partial y}\left(e^{-\gamma\theta}\frac{\partial v}{\partial y}\right)-\frac{e^{-\gamma\theta}}{K}v, \tag{11}$$

$$\frac{\partial u}{\partial x}+\frac{\partial v}{\partial y}=0, \tag{12}$$

$$Pr\left(u\frac{\partial\theta}{\partial x}+v\frac{\partial\theta}{\partial y}\right)=\omega\left(\frac{\partial^2\theta}{\partial x^2}+\frac{\partial^2\theta}{\partial y^2}\right)-\alpha\theta, \tag{13}$$

with the following boundary conditions:

$$\left.\begin{aligned} &u=0, \quad v=0, \quad \theta=1, \quad \text{at} \quad y=\varepsilon\cos(\lambda x),\\ &u=0, \quad v=0, \quad \frac{\partial\theta}{\partial y}=0, \quad \text{at} \quad y=1+\varepsilon\cos(\lambda x), \end{aligned}\right\} \tag{14}$$

where $\omega=(1+(4/3R))$ is the radiation parameter.

Taking the Maclaurin's expansion of the exponential terms in Eqs. (10) and (11), which can be expressed as

$$e^{-\gamma\theta}=1-\gamma\theta+O(\gamma^2). \tag{15}$$

Assuming that the solution consists of a mean part and a perturbed part, the velocity and temperature distributions are

$$\left.\begin{aligned} &u(x,y)=u_0(y)+\varepsilon u_1(x,y),\\ &v(x,y)=\varepsilon v_1(x,y),\\ &\theta(x,y)=\theta_0(y)+\varepsilon\theta_1(x,y),\\ &p(x,y)=p_0(x)+\varepsilon p_1(x,y), \end{aligned}\right\} \tag{16}$$

where the perturbed quantities u_1,v_1,θ_1 and p_1 are small compared the mean quantities.

Substituting Eqs. (15) and (16) into Eqs. (10)–(13) with boundary conditions (15), we obtained the following sets of equations:

For zeroth order equations, we are:

$$(1-\gamma\theta_0)\frac{d^2u_0}{dy^2}-\gamma\frac{du_0}{dy}\frac{d\theta_0}{dy}-Mu_0-\frac{(1-\gamma\theta_0)}{K}u_0=-G\theta_0-C, \tag{17}$$

$$\omega\frac{d^2\theta_0}{dy^2}-\alpha\theta_0=0, \tag{18}$$

with corresponding boundary condition

$$\left.\begin{aligned} &u_0=0, \quad \theta_0=1, \quad y=0,\\ &u_0=0, \quad \frac{d\theta_0}{dy}=0, \quad y=1, \end{aligned}\right\} \tag{19}$$

and for first order equations, we obtain:

$$\begin{aligned} u_0\frac{\partial u_1}{\partial x}+v_1\frac{du_0}{dy}=\;& -\frac{\partial p_1}{\partial x}+(1-\gamma\theta_0)\frac{\partial^2u_1}{\partial x^2}+(1-\gamma\theta_0)\frac{\partial^2u_1}{\partial y^2}-\gamma\frac{du_0}{dy}\frac{\partial\theta_1}{\partial y}\\ &-\gamma\frac{d\theta_0}{dy}\frac{\partial u_1}{\partial y}+G\theta_1-Mu_1-\frac{(1-\gamma\theta_0)}{K}u_1, \end{aligned} \tag{20}$$

$$u_0\frac{\partial v_1}{\partial x}=-\frac{\partial p_1}{\partial y}+(1-\gamma\theta_0)\frac{\partial^2v_1}{\partial x^2}+(1-\gamma\theta_0)\frac{\partial^2v_1}{\partial y^2}-\gamma\frac{d\theta_0}{dy}\frac{\partial v_1}{\partial y}-\frac{(1-\gamma\theta_0)}{K}v_1, \tag{21}$$

$$\frac{\partial u_1}{\partial x}+\frac{\partial v_1}{\partial y}=0, \tag{22}$$

$$Pr\left(u_0\frac{\partial\theta_1}{\partial x}+v_1\frac{\partial\theta_0}{\partial y}\right)=\omega\left(\frac{\partial^2\theta_1}{\partial x^2}+\frac{\partial^2\theta_1}{\partial y^2}\right)-\alpha\theta_1, \tag{23}$$

with boundary conditions

$$\left.\begin{aligned} &u_1=-\frac{du_0}{dy}\cos(\lambda x), \quad v_1=0, \quad \theta_1=-\frac{d\theta_0}{dy}\cos(\lambda x), \quad y=0,\\ &u_1=0, \quad v_1=0, \quad \frac{\partial\theta_1}{\partial y}=0, \quad y=1, \end{aligned}\right\} \tag{24}$$

where $C = -\frac{dp_0}{dx}$ is taken to be zero.

Eqs. (20)–(23) with boundary conditions (24) are simplified by introducing the stream function $\Psi(x, y)$ such that

$$u_1 = -\frac{\partial \Psi}{\partial y}, \; v_1 = \frac{\partial \Psi}{\partial x}. \tag{25}$$

Note that Eq. (22) is satisfied identically and eliminating p_1 from (20) and (21), reduce to

$$u_0\left(\frac{\partial^3 \Psi}{\partial x^3} + \frac{\partial^3 \Psi}{\partial x \partial y^2}\right) - \frac{d^2 u_0}{dy^2}\frac{\partial \Psi}{\partial y} - (1-\gamma\theta_0)\frac{\partial^4 \Psi}{\partial x^4} - (1-\gamma\theta_0)\frac{\partial^4 \Psi}{\partial y^4} - 2(1-\gamma\theta_0)\frac{\partial \Psi^4}{\partial x^2 \partial y^2} - \gamma\frac{d^2 u_0}{dy^2}\frac{\partial \theta_1}{\partial y}$$
$$+\gamma\frac{d\theta_0}{dy}\frac{\partial^3 \psi}{\partial y \partial x^2} + \gamma\frac{d\theta_0}{dy}\frac{\partial^2 \psi}{\partial y^2} + M\frac{\partial^2 \Psi}{\partial y^2} + \frac{(1-\gamma\theta_0)}{K}\left(\frac{\partial^2 \Psi}{\partial y^2} + \frac{\partial^2 \Psi}{\partial x^2}\right) - G\frac{\partial \theta_1}{\partial y} = 0, \tag{26}$$

$$Pr\left(u_0\frac{\partial \theta}{\partial x} + \frac{\partial \Psi}{\partial x}\frac{\partial \theta_0}{\partial y}\right) = \omega\left(\frac{\partial^2 \theta_1}{\partial x^2} + \frac{\partial^2 \theta_1}{\partial x^y}\right) - \alpha\theta_1. \tag{27}$$

with boundary conditions

$$\left.\begin{aligned} &\frac{\partial \Psi}{\partial y} = -\frac{du_0}{dy}\cos(\lambda x), \quad \frac{\partial \Psi}{\partial x} = 0, \quad \theta_1 = -\frac{d\theta_0}{dy}\cos(\lambda x), \quad y = 0. \\ &\frac{\partial \Psi}{\partial y} = 0, \quad \frac{\partial \Psi}{\partial x} = 0, \quad \frac{\partial \theta_1}{\partial y} = 0, \qquad\qquad\qquad\quad y = 1. \end{aligned}\right\} \tag{28}$$

Due to the nature of the wall motion, we use complex exponential series of wave plane equation

$$\Psi(x, y) = Real\left[\sum_r (\psi_r \lambda^r e^{(i\lambda x)})\right], \tag{29}$$

$$\theta_1(x, y) = Real\left[\sum_r (t_r \lambda^r e^{(i\lambda x)})\right], \tag{30}$$

where $r = 0, 1$.

Substituting Eqs. (29) and (30) into Eqs. (26) and (27) with boundary conditions (28), we obtain the following sets of ordinary differential equations:

$$(1-\gamma\theta_0)\frac{d^4\psi_0}{dy^4} + \gamma\frac{dt_0}{dy}\frac{d^2 u_0}{dy^2} - \gamma\frac{d^2\psi_0}{dy^2}\frac{d\theta_0}{dy} - M\frac{d^2\psi_0}{dy^2} - \frac{(1-\gamma_0)}{K}\frac{d^2\psi_0}{dy^2} = G\frac{dt_0}{dy}, \tag{31}$$

$$\omega\frac{d^2 t_0}{dy^2} - \alpha t_0 = 0, \tag{32}$$

$$(1-\gamma\theta_0)\frac{d^4\psi_1}{dy^4} + \gamma\frac{dt_1}{dy}\frac{d^2 u_0}{dy^2} - \gamma\frac{d^2\psi_1}{dy^2}\frac{d\theta_0}{dy} - M\frac{d^2\psi_1}{dy^2} - \frac{(1-\gamma_0)}{K}\frac{d^2\psi_1}{dy^2} - i\left(\psi_0\frac{d^2 u_0}{dy^2} - u_0\frac{d^2\psi_0}{dy^2}\right) = G\frac{dt_1}{dy}, \tag{33}$$

$$\omega\frac{d^2 t_1}{dy^2} - \alpha t_1 = i\,Pr\left(u_0 t_0 + \psi_0\frac{d\theta_0}{dy}\right), \tag{34}$$

with corresponding boundary conditions

$$\left.\begin{aligned} &\psi_0' = -u_0', \quad \psi_0 = 0, \quad t_0 = -\theta_0', \quad y = 0, \\ &\psi_0' = 0, \quad \psi_0 = 0, \quad t_0\prime = 0, \qquad\quad y = 1, \end{aligned}\right\} \tag{35}$$

$$\left.\begin{aligned} &\psi_1' = 0, \quad \psi_1 = 0, \quad t_1 = 0, \quad y = 0, \\ &\psi_1' = 0, \quad \psi_1 = 0, \quad t_1\prime = 0, \quad y = 1. \end{aligned}\right\} \tag{36}$$

3. Differential Transform Method of solution

We transformed differential Eqs. (17), (18), (31)–(34) with boundary conditions (19), (35) and (36) in the following forms as [27,28]

$$\begin{aligned} U_0(k+2) = \frac{k!}{(k+2)!}\Bigg(&\gamma\sum_{r=0}^{k}(k-r+1)(k-r+2)\theta_0(r)U_0(k-r+2) \\ &+\gamma\sum_{r=0}^{k}(r+1)(k-r+1)\theta_0(r+1)U_0(k-r+1) + MU_0(k) + \frac{1}{K}U_0(k) \\ &-\frac{\gamma}{K}\left(\sum_{r=0}^{k}\theta_0 U_0(k-r)\right) - G\theta_0(k)\Bigg), \end{aligned} \tag{37}$$

$$\theta_0(k+2) = \frac{k!}{(k+2)!}\left(\frac{\alpha\theta_0(k)}{\omega}\right), \tag{38}$$

with corresponding boundary conditions

$$\left.\begin{aligned} &U_0 = 0, \quad \theta_0 = 1, && y = 0, \\ &\sum_{k=0}^{n}U_0(k) = 0, \quad \sum_{k=0}^{n}k\theta_0(k) = 0, && y = 1, \end{aligned}\right\} \tag{39}$$

$$\begin{aligned} \psi_0(k+4) = \frac{k!}{(k+4)!}\Bigg(&\gamma\sum_{r=0}^{k}(k-r+1)(k-r+2)(k-r+3)(k-r+4)\theta_0(r)\psi_0(k-r+4) \\ &-\gamma\sum_{r=0}^{k}(r+1)(k-r+1)(k-r+2)T_0(r+1)\psi_0(k-r+2) \\ &+\gamma\sum_{r=0}^{k}(r+1)(k-r+1)(k-r+2)\theta_0(r+1)\psi_0(k-r+2) + M\frac{(k+2)}{k!}\psi_0(k+2) \\ &+\frac{(k+2)!}{k!}\frac{1}{K}\psi_0(k+2) - \frac{\gamma}{K}\sum_{r=0}^{k}(k-r+1)(k-r+2)\theta_0(r)\psi_0(k-r+2) \\ &+\frac{(k+1)!}{k!}GT_0(k+1)\Bigg), \end{aligned} \tag{40}$$

$$T_0(k+2) = \frac{k!}{(k+2)!}\left(\frac{\alpha T_0(k)}{\omega}\right), \tag{41}$$

together with boundary conditions

$$\left.\begin{aligned} &\psi_0 = U_0(k), \quad \psi_0(1) = 0, \quad T_0 = -\theta_0\prime(k), && y = 0, \\ &\sum_{k=0}^{n}k\psi_0(k) = 0, \quad \sum_{k=0}^{n}\psi_0(k) = 0, \quad \sum_{k=0}^{n}kT_0(k) = -\theta_0''(k), && y = 1. \end{aligned}\right\} \tag{42}$$

Also,

$$\psi_1(k+4) = \frac{k!}{(k+4)!}\left(\gamma\sum_{r=0}^{k}(k-r+1)(k-r+2)(k-r+3)(k-r+4)\theta_0(r)\psi_1(k-r+4)\right.$$
$$-\gamma\sum_{r=0}^{k}(r+1)(k-r+1)(k-r+2)T_1(r+1)\psi_1(k-r+2)$$
$$+\gamma\sum_{r=0}^{k}(r+1)(k-r+1)(k-r+2)\theta_0(r+1)\psi_1(k-r+2)$$
$$+M\frac{(k+2)}{k!}\psi_1(k+2)+\frac{(k+2)!}{k!}\frac{1}{K}\psi_1(k+2)$$
$$-\frac{\gamma}{K}\sum_{r=0}^{k}(k-r+1)(k-r+2)\theta_0(r)\psi_1(k-r+2)+\frac{(k+1)!}{k!}GT_0(k+1)$$
$$+i\left(\sum_{r=1}^{k}(k-r+1)(k-r+2)U_0\psi_0(k-r+2)\right.$$
$$\left.\left.-\gamma\sum_{r=0}^{k}(k-r+1)(k-r+2)\psi_0U_0(k-r+2)\right)\right), \tag{43}$$

$$T_1(k+2) = \frac{k!}{(k+2)!}\left(\frac{\alpha T_1(k)}{\omega}+iPr\sum_{r=0}^{k}U_0(k)T_0(k-r)+iPr\sum_{r=0}^{k}(k+1)(k+2)\theta_0(k)\psi_0(k-r)\right), \tag{44}$$

with the boundary conditions

$$\left.\begin{aligned}&\psi_1(0)=0,\quad \psi_1(1)=0,\quad T_1=0, && y=0,\\ &\sum_{k=0}^{n}k\psi_1(k)=0,\quad \sum_{k=0}^{n}\psi_1(k)=0,\quad \sum_{k=0}^{n}kT_1(k)=0, && y=0,\end{aligned}\right\} \tag{45}$$

The perturbed velocity u_1 and the perturbed temperature θ_1 can now be expressed (Teneja and Jain [22]) follows:

$$u_1 = -\left[\psi_r{}'\cos(\lambda x)-\lambda\psi_i{}'\sin(\lambda x)\right], \tag{46}$$

$$\theta_1 = \left[t_r\cos(\lambda x)-\lambda t_i\sin(\lambda x)\right], \tag{47}$$

The transformed equations were solved with corresponding boundary conditions using Maple symbolic package 17 to obtained θ_0, θ_1, and velocity u_0, u_1.

3.1. Skin friction and Nusselt number

3.1.1. Skin friction

The shear stress on the wavy boundaries, $y=\varepsilon\cos(\lambda x)$ and $y=1+\varepsilon\cos(\lambda x)$ are given as

$$\tau = u\prime(0)+\varepsilon(-\psi_r''(0)\cos(\lambda x)+\lambda\psi_i''(0)\sin(\lambda x)), \tag{48}$$

$$\tau = u\prime(1)+\varepsilon(-\psi_r''(1)\cos(\lambda x)+\lambda\psi_i''(1)\sin(\lambda x)). \tag{49}$$

3.1.2. Nusselt number

The rate of heat transfer at the wavy boundaries, $y=\varepsilon\cos(\lambda x)$ and $y=1+\varepsilon\cos(\lambda x)$ are given as

$$Nu = -\theta\prime(0)-\varepsilon\left(-t_r\prime(0)\cos(\lambda x)+\lambda t_i\prime(0)\sin(\lambda x)\right), \tag{50}$$

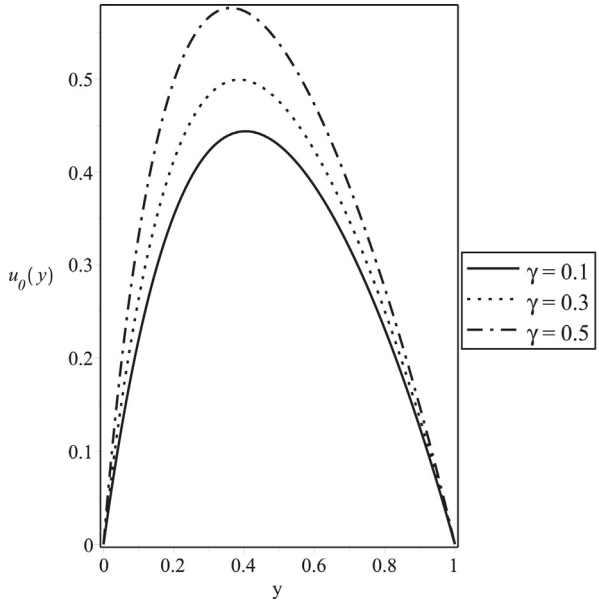

Fig. 1. Zeroth-order velocity profiles for different values of γ.

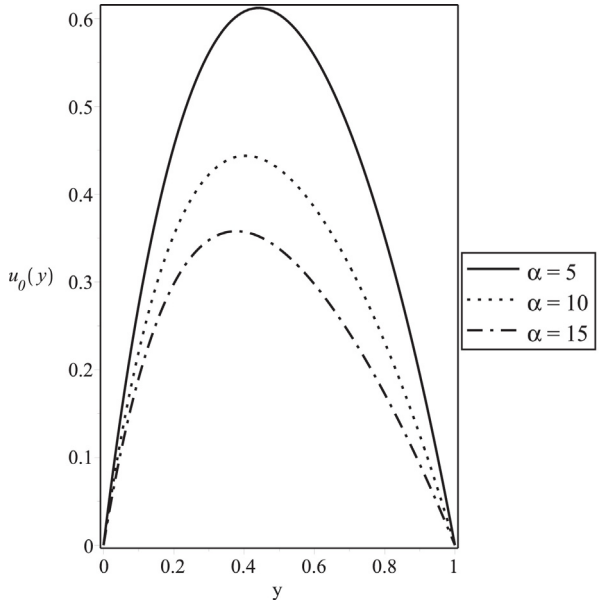

Fig. 2. Zeroth-order velocity profiles for different values of α.

$$Nu = -\theta\prime(1) - \varepsilon(-t_r\prime(1)\cos(\lambda x) + \lambda t_i\prime(1)\sin(\lambda x)). \tag{51}$$

4. Discussion of results

A series of computations has been carried out on the effects of the following parameters: variable viscosity parameter (γ), heat source (α), radiation parameter (ω), Hartmann number (M), Grashof number (G), permeability parameter (K), frequency (λ) and epsilon (ε) on the velocity, temperature, skin friction as well as Nusselt number. The results of the present analysis are of two categories: zeroth-order and first-order results.

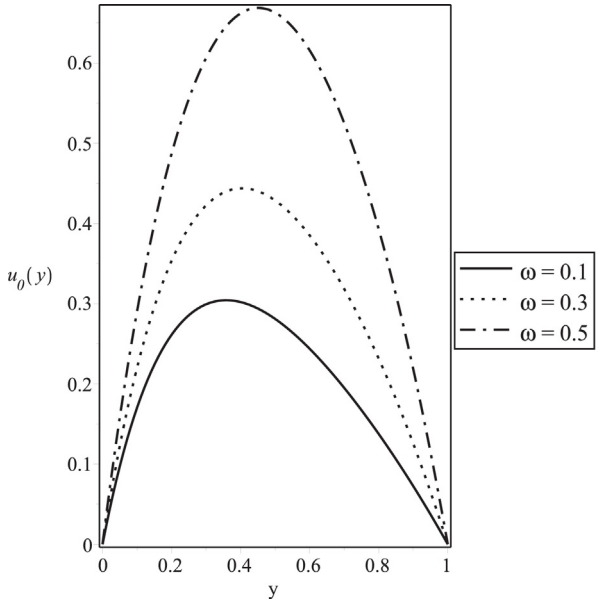

Fig. 3. Zeroth-order velocity profiles for different values of ω.

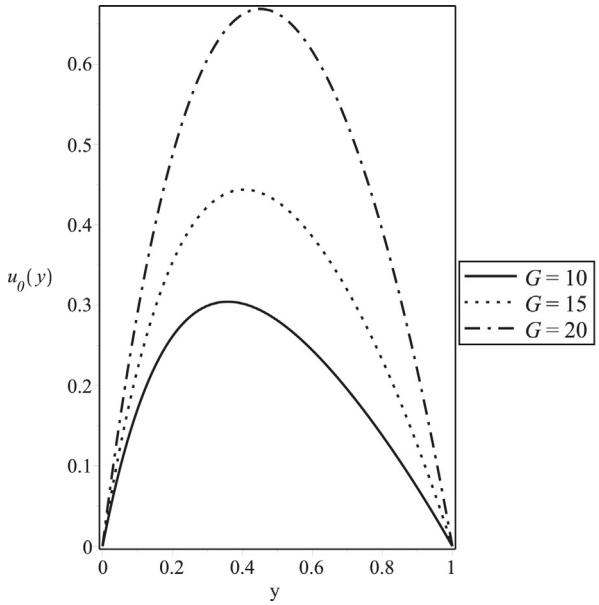

Fig. 4. Zeroth-order velocity profiles for different values of G.

4.1. Zeroth-order solution

The analysis of the fluid flow for zeroth-order distribution profiles uses the default values for the parameters: $\gamma = 0.1$, $\alpha = 10$, $\omega = 2$, $M = 1$, $G = 10$ and $K = 1$. All the graphs correspond to the default values expect otherwise stated on the graphs.

Fig. 1 illustrates the zeroth-order velocity distribution profiles with variation of variable viscosity parameter. It is observed that an increase in variable viscosity parameter reduces the shear or bulk viscosity which decreases the fluid's resistance to flow, thus increasing the velocity of the fluid.

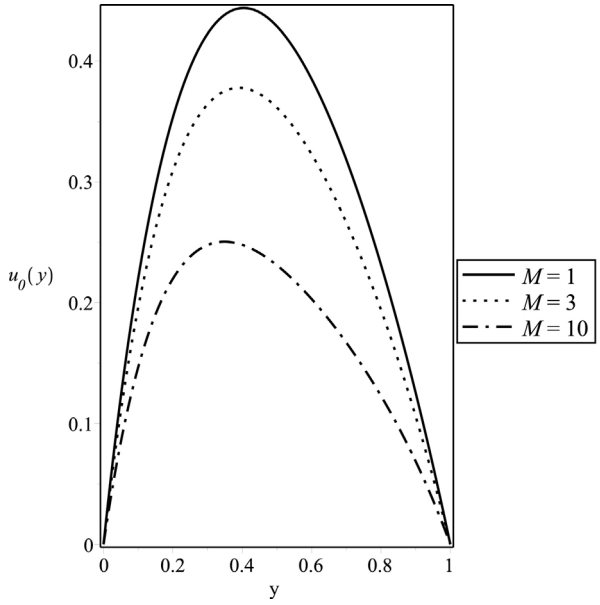

Fig. 5. Zeroth-order velocity profiles for different values of M.

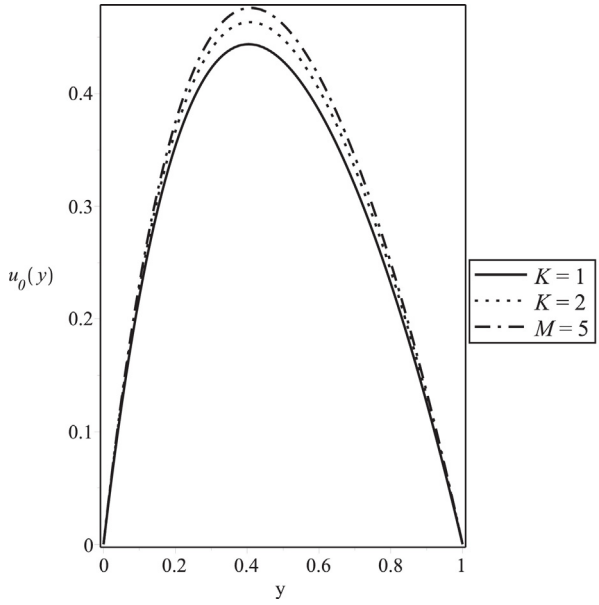

Fig. 6. Zeroth-order velocity profiles for different values of K.

Fig. 2 depicts the zeroth-order velocity distribution profiles with different values of heat source parameter. It can be seen that an increase in heat source parameter causes a reduction in the buoyancy effect of the boundary layer which reduces the fluid velocity.

Fig. 3 shows the influence of radiation parameter on the zeroth-order velocity profiles. It is observed that as the radiation parameter increases, thereby increasing the momentum of the boundary layer thickness. This is because, when the intensity of heat generated through thermal radiation increased, the bond-holding the component of the fluid particles together easily broken and the fluid velocity increased.

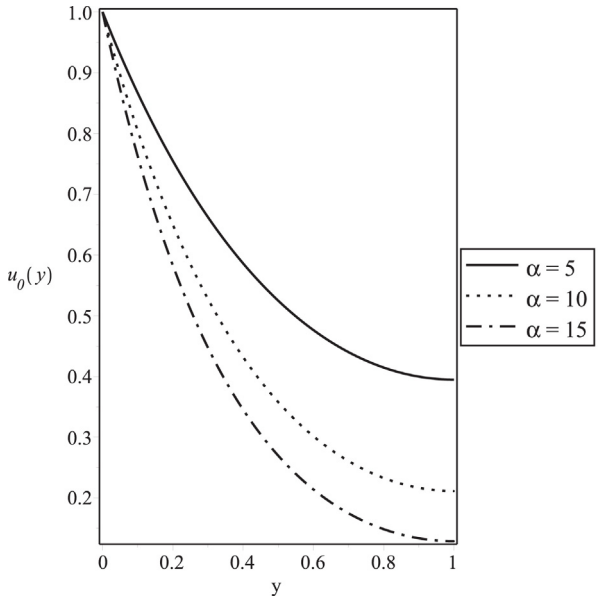

Fig. 7. Zeroth-order temperature profiles for different values of α.

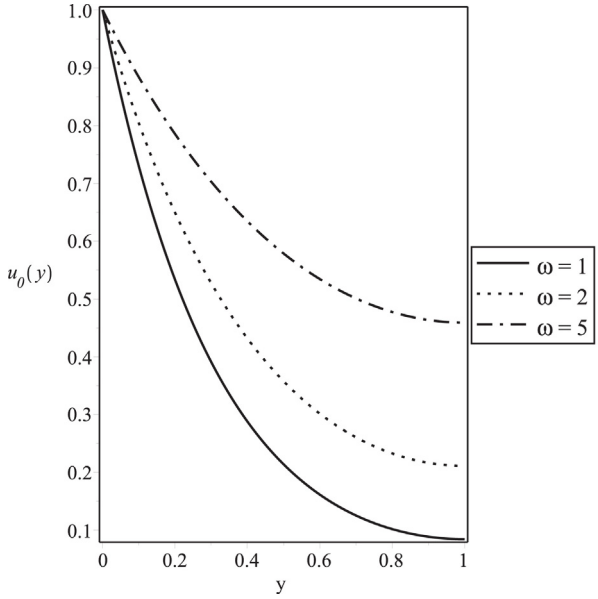

Fig. 8. Zeroth-order temperature profiles for different values of ω.

The effects of Grashof number are presented in Fig. 4. It can be seen that an increase in Grashof number significantly increases the boundary layer thickness which resulted in the rapidly enhancement of the fluid velocity. It agrees with the fact that the effects of increasing the Grashof are to increase the values of the velocity profile.

Fig. 5 illustrates the zeroth-order velocity profiles with variation of magnetic parameter. It is observed that the presence of magnetic field produces retard force on the fluid flow. This force is called Lorentz force, which slow down the fluid velocity

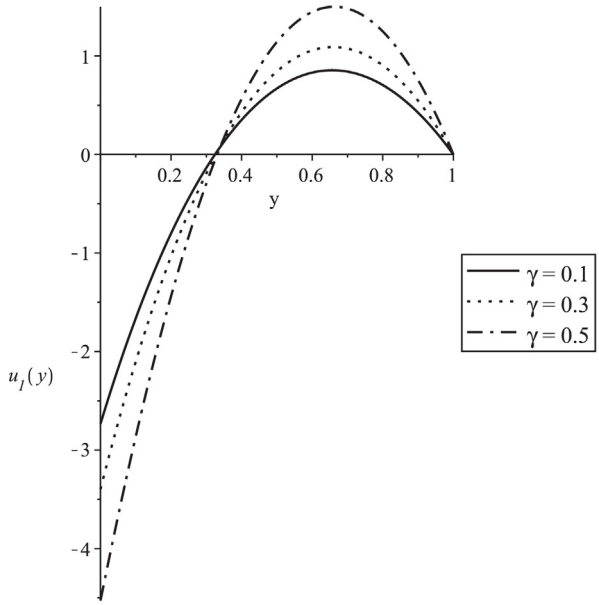

Fig. 9. First-order velocity profiles for different values of γ.

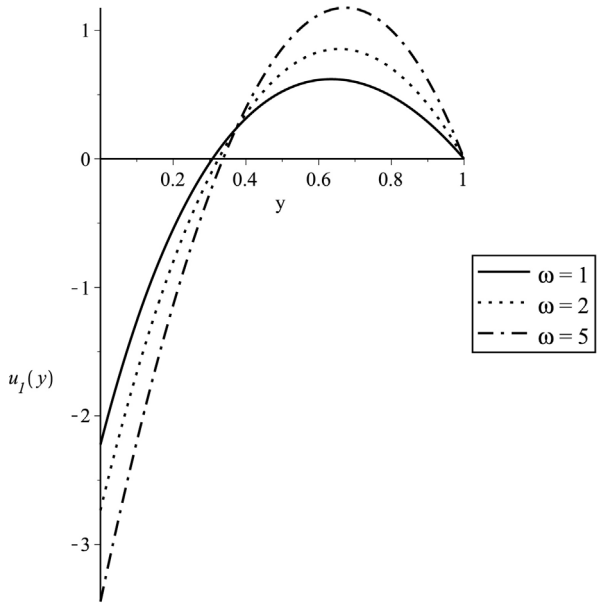

Fig. 10. First-order velocity profiles for different values of ω.

Fig. 6 presents the zeroth-order velocity distribution with variation of permeability parameter. It shows that the presence of permeability parameter reduces the resistance of the porous medium which enhance the fluid velocity.

Figs. 7 and 8 illustrate zeroth-order temperature distribution profile with variation of radiation parameter and heat source parameter. It can be seen that an increase in the radiation parameter significantly increases the temperature profile. While an increase in the heat source parameter significantly decreases the thermal buoyancy effects which reduces the fluid temperature.

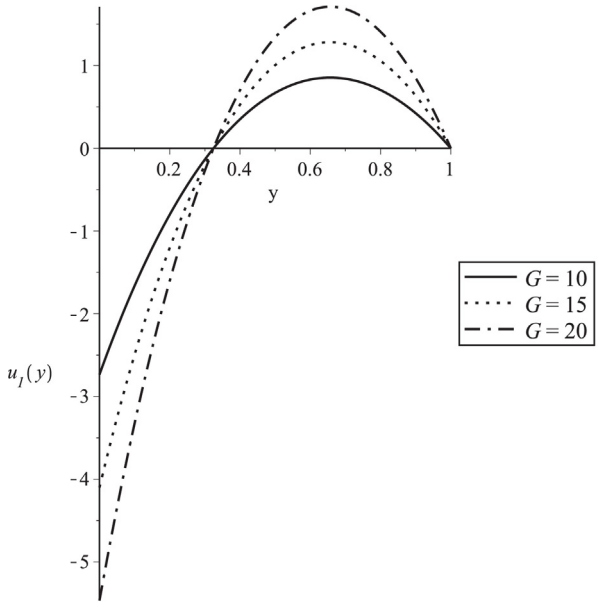

Fig. 11. First-order velocity profiles for different values of G.

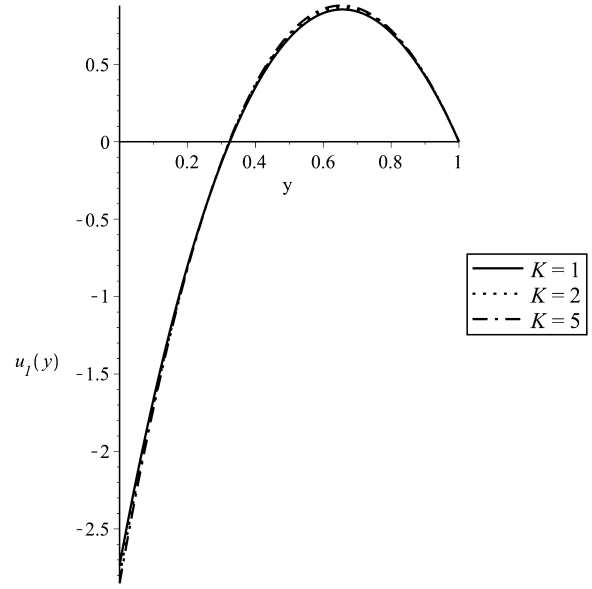

Fig. 12. First-order velocity profiles for different values of K.

4.2. First order

The analysis of the fluid flow for first-order distribution profiles uses the default values for the parameters: $\gamma = 0.1$, $\alpha = 10$, $\omega = 2$, $M = 1$, $G = 10$, $K = 1$, $\lambda = 0.01$, $\varepsilon = 0.01$ and $x = 1$. All the graphs correspond to the default values expect otherwise stated on the graphs.

Figs. 9 and 10 depict the first-order velocity distribution profiles with variation of variable viscosity parameter and radiation parameter respectively. It is observed that an increase either variable parameter or radiation parameter slow down the first order profiles within the range $0 \leq y \leq 0.32$, but speed up the first velocity profiles within the range

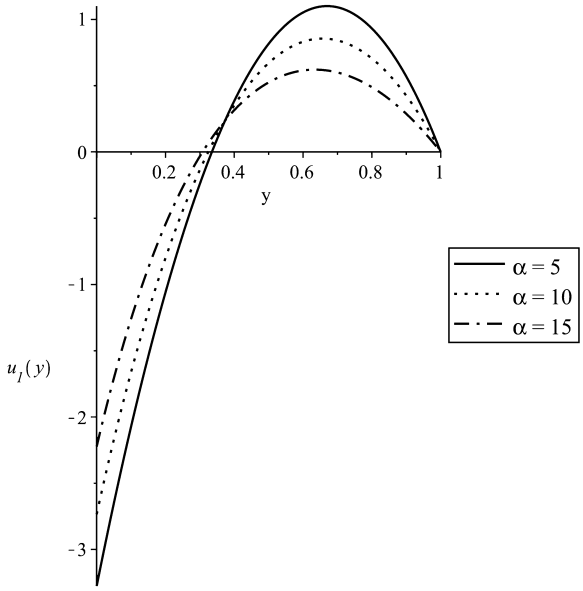

Fig. 13. First-order velocity profiles for different values of α.

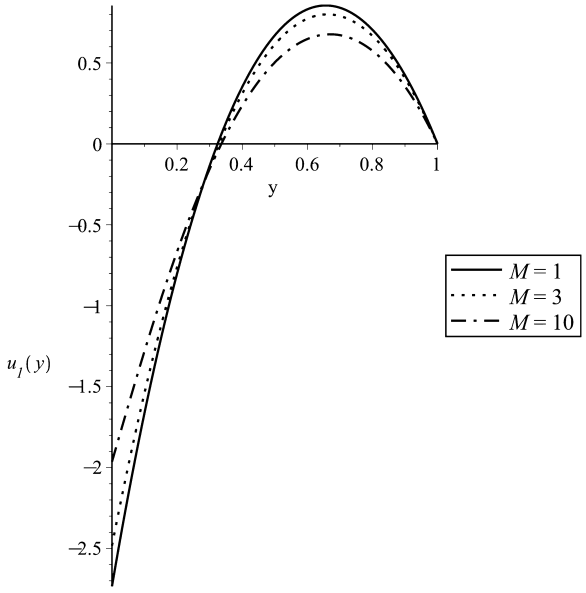

Fig. 14. First-order velocity profiles for different values of M.

$0.32 \leq y \leq 1$. It is because an increase variable viscosity parameter reduces the bulk viscosity, thereby increasing the fluid velocity. The presence of radiation parameter increases buoyancy force which increases the fluid velocity.

Figs. 11 and 12 illustrate variation of Grashof number (G) and permeability parameter on the first-order velocity respectively. It can be seen that an increase in thermal Grashof number decreases the first order profiles within the range $0 \leq y \leq 0.38$, but increases the first order velocity profile within the range $0.38 \leq y \leq 1$. The permeability of the porous medium has no significant effect on the first order velocity profiles.

Fig. 13 depicts the first-order velocity distribution profile with variation of heat source parameter. It can been seen that increase in the heat source significantly increases the first order velocity profiles within the range $0 \leq y \leq 0.36$ while the first velocity profiles reduces with the range $0.36 \leq y \leq 1$.

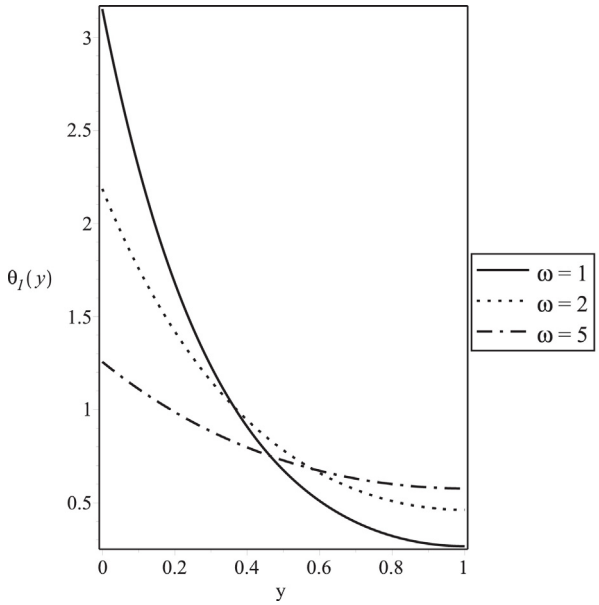

Fig. 15. First-order temperature profiles for different values of ω.

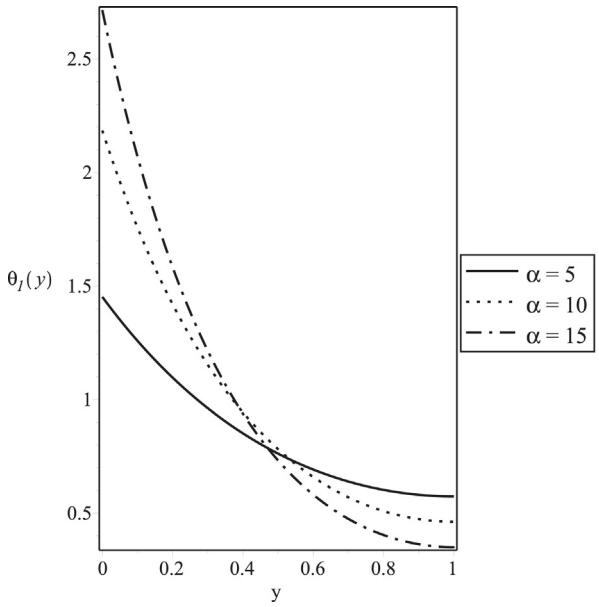

Fig. 16. First-order temperature profiles for different values of α.

Fig. 14 illustrates the influence of magnetic parameter (M) on the first order velocity profile. It is observed that the increase in magnetic field parameter increases velocity profiles within the range $0 \leq y \leq 0.34$, but it reduces the first order velocity profiles within the range $0.34 \leq y \leq 1$.

Figs. 15 and 16 illustrate the first-order temperature profile with variation of heat source parameter and radiation parameter respectively. It is seen that an increase in radiation parameter causes a fall in the temperature profiles within the range $0 \leq y \leq 0.42$, but it produces a rise in the fluid temperature profiles. While an increases in heat source parameter causes a drop in the temperature profile within $0 \leq y \leq 0.42$, but it causes a fall in the fluid temperature profiles.

The skin friction coefficient and Nusselt number are expressed in Eqs. (48)–(51) and are shown in Tables 1 and 2 for various values of fluid parameters. In order to highlight the contributions of each parameter, one parameter is varied

Table 1
The skin friction coefficients for various values of γ, α, ω, M, G and K.

Fluid parameters	$y=0$	$y=1$
$\gamma=0.1$	6.0019	−5.1127
$\gamma=0.3$	6.4238	−5.8610
$\gamma=0.5$	6.9128	−6.7280
$\alpha=1$	5.6323	−5.6951
$\alpha=3$	5.7434	−5.4151
$\alpha=5$	6.0019	−5.1127
$\omega=0.3$	9.0756	−1.9869
$\omega=0.5$	5.7435	−5.1127
$\omega=0.7$	5.6718	−5.4150
$M=1$	6.2392	−5.1127
$M=3$	6.0019	−4.5618
$M=5$	5.1884	−1.0914
$G=10$	2.9743	−2.5307
$G=15$	6.0019	−5.1127
$G=20$	12.0571	−10.2756
$K=1$	5.9375	−5.1026
$K=3$	5.9254	−5.14992
$K=5$	5.9240	−5.5678

Table 2
The Nusselt number for various values of α and ω.

Fluid parameters	$y=0$	$y=1$
$\alpha=1$	2.9998×10^{-8}	24.1966
$\alpha=2$	-1.0999×10^{-7}	69.9509
$\alpha=5$	-1.0×10^{-7}	227.8422
$\omega=0.1$	8.9995×10^{-8}	52.2527
$\omega=0.3$	2.9998×10^{-8}	24.1965
$\omega=0.5$	4.0×10^{-9}	15.1363

while the rest take default fixed values. It is observed from Table 1 that an increase in any of the parameter γ, α and G produces a rise in the skin friction while increase in any of parameter ω, M and K resulted in reduction in the skin friction coefficient at the wall $y=0$. It can be seen that an increase in any of parameter γ, ω, G and K causes a reduction of the skin friction while increase in α or M increases the skin friction at the wall $y=1$.

As for the Nusselt number shown in Table 2, an increase in heat source (α) increase the Nusselt number while an increase in ω cause a reduction in the Nusselt number at the wall $y=0$. It is observed that an increase in heat source α increases the Nusselt number while an increase ω decreases in the Nusselt number at the wall $y=1$.

5. Conclusion

The effects of variable viscosity on radiative MHD free convection flow in a porous medium between two vertical wavy walls are presented. The resulting governing equations from the mathematical model of the problem are non-dimensionalised, simplified using perturbation technique and complex exponential series for plane equation, and solved using Differential Transform Method (DTM). A series of computations was carried out to study the effects of the fluid parameters such as variable parameter viscosity (γ), radiation parameter (ω), heat source (α), magnetic parameter (M), Grashof number (Gr) and the permeability parameter (K) on the velocity, temperature, skin friction as well as Nusselt number.

The followings were observed:

(i) An increase in any of variable viscosity parameter, radiation, Grashoff number and the permeability parameter produces a rise in the velocity profile while an increase in heat source or Hartmann number causes a reduction in the velocity profile on the zeroth distribution profile.
(ii) An increase in radiation increases zeroth-temperature. Whereas an increase in heat source has a retard effect on the zeroth-order temperature profile.
(iii) An increase in temperature dependent parameter, radiation parameter, Grashoff number and the permeability parameter, increases the first-order velocity while an increase in heat source and magnetic field cause a reduction on the first-order velocity.
(iv) As radiation increases the first order temperature increase. Whereas the first temperature increases as the heat source increases.
(v) there is a rise in the skin friction due to an increase in any of γ, ω, G and K while a fall is observed in skin friction with an increase in M or α at the wall $y = 0$.
(vi) An increase in any of γ, ω, G and K causes a reduction in the skin friction while an increase in α or M produces a rise in the skin friction.
(vii) Finally, there is an increase in the Nusselt number as α increases while decrease in the Nusselt number as ω increases at both walls.

Acknowledgement

The authors appreciate and acknowledge the contributions of the reviewers to make the article robust.

References

[1] M.K. Chaube, S.K. Pandey, D. Tripathi, Slip effect on peristaltic transport of micropolar fluid, Appl. Math. Sci. 4 (43) (2010) 2015–2117.
[2] N.S. Akbar, A.W. Butt, Physiological transportation of Casson fluid in a plumb duct, Commun. Theor. Phys. 65 (2015) 347–352.
[3] A.M. Siddiqui, A.A. Farooq, M.A. Rana, A mathematical model for the flow of a Casson fluid due metachronal beating of cilia in tube, Sci. World J. 2015 (2015), http://dx.doi.org/10.1155/2015/487819.
[4] N.S. Akbar, Natural convective MHD peristaltic flow of a nanofluid with convective surface boundary conditions, J. Comput. Theor. Nanosci. 12 (6) (2015) 257–262.
[5] N.S. Akbar, Bioconvection peristaltic flow in an asymmetric channel filled by nanofluid containing gyrotactic micro-organism. Bio-nano engineering model, Int. J. Numer. Methods Heat Fluid Flow 25 (2015) 214–224.
[6] N.S. Akbar, Z.H. Khan, Metachronal beating of cilia under the influence of Casson fluid and magnetic field, J. Magn. Magn. Mater. 378 (2015) 320–325.
[7] N.S. Akbar, Influence of magnetic field on peristaltic flow of a Casson fluid in an asymmetric channel: application in crude oil refinement, J. Magn. Magn. Mater. (2015) 463–468.
[8] S.G. Lekoudis, A.H. Neyfeh, W.S. Saric, Compressible boundary layers over wavy walls, Phys. Fluids (1976) 514–519.
[9] P.N. Shankar, U.N. Sinha, The Rayleigh problem for a wavy wall, J. Fluid Mech. 77 (1976) 243–256.
[10] M. Lessen, S.T. Gangwani, Effect of small amplitude wall waviness upon the stability of the laminar boundary layer, Phys. Fluid 19 (1976) 510–513.
[11] K. Vajravelu, K.S. Sastri, Free convection heat transfer in a viscous incompressible fluid confined between a long vertical wavy and a parallel flat wall, J. Fluid Mech. 86 (2) (1978).
[12] U.N. Das, N. Ahmed, Free convective MHD flow and heat transfer in a viscous incompressible fluid confined between a long wavy wall and parallel flat wall, Indian J. Pure Appl. Math. 23 (4) (1992) 295–304.
[13] P.F. Fasogbon, MHD flows in corrugated channel, Int. Pure Appl. Math. 27 (2) (2006) 225–237.
[14] S.S. Tak, H. Kumar, Heat transfer with radiation in MHD free convection flow confined between a vertical wavy wall and a flat wall, Bull. Pure Appl. Math. 1 (2) (2007) 126–140.
[15] P.F. Fasogbon, Analytical studies of heat and mass transfer by convection in a two dimensional irregular channel, Int. J. Appl. Math. Mech. 6 (4) (2010) 17–37.
[16] J.U. Abubakar, Natural convective flow and heat transfer in a viscous incompressible with slip effects confined within spirally-enhanced channel, Univ. Ilorin, 2014 (unpublished Ph.D. thesis).
[17] S.S. Tak, H. Kumar, MHD free convection flow with viscous dissipation in a vertical wavy channel, Ultra Sci. Phys. Sci. 18 (2M) (2006) 221–232.
[18] H. Kumar, Heat transfer with radiation and temperature dependent heat source in MHD free convection flow confined between two vertical wavy walls, Int. J. Appl. Math. Mech. 7 (2) (2011) 77–103.

[19] S.O. Adesanya, O.D. Makinde, MHD oscillatory slip flow and heat transfer in a channel filled with porous media, U.P.B. Sci. Bull. Ser. A 76 (1) (2014) 197–204.
[20] G. Makanda, O.D. Makinde, P. Sibanda, Natural convection of viscoelastic fluid from a cone embedded in a porous medium with viscous dissipation, Math. Probl. Eng. (2014) 934712.
[21] S. Das, R.N. Jana, O.D. Makinde, An oscillatory MHD convective flow in vertical channel filled with porous medium with hall and thermal radiation effects, Spec. Top. Rev. Porous Medium 5 (1) (2014) 63–82.
[22] R. Teneja, N.C. Jain, MHD flow with slip effects and temperature dependent heat source in a viscous incompressible fluid confined between a long vertical wavy wall and a parallel flat wall, Defense Sci. J. 20 (4) (2004) 327–340.
[23] M.S. Dada, A.B. Disu, Heat transfer with radiation and temperature heat dependent source in MHD free convection flow in porous medium between two vertical walls, J. Nigeria Math. Soc. (2014), http://dx.doi.org/10.1016/j.jnnms.2014.12.
[24] H. Herwig, K. Gersten, Warme Stafubertr 20 (4) (1986).
[25] M.N. Ozisik, Radiation Transfer and Interactions with Conduction and Convection, Wiley-Inter-science Publication, USA, 1973.
[26] M.Q. Brewster, Thermal Radiative Transfer and Properties, John Wiley and Sons Inc., New York, USA, 1992.
[27] H.I. Abdel-Halim, S.E. Vedat, Solution of different types of the linear and nonlinear higher order boundary value problems by Differential Transform Method, Eur. J. Pure Appl. Math. 2 (3) (2009) 426–447.
[28] J.K. Zhou, Differential Transformation and Its Applications for Electrical Circuits, Huarjung Univ. Press, Wuhan, China, 1986.